The 1999 T.R. Higgins Lecture: Design of Reduced Beam Section Moment Connections

Michael D. Engelhardt

Author

Michael D. Engelhardt is an associate professor of civil engineering at the University of Texas at Austin. He received his bachelor of science and master of science degrees in civil engineering from the University of Illinois at Urbana and a Ph.D. from the University of California at Berkeley. Between his master and Ph.D. degrees, he worked as a project engineer for Exxon Research and Engineering Company in Florham Park, New Jersey. Dr. Engelhardt joined the faculty at the University of Texas in 1989.

Dr. Engelhardt teaches courses on structural steel design at the University of Texas and conducts research on seismic-resistant steel framing. His previous work includes contributions on steel eccentrically braced frames and moment resisting frames. He has been an active participant in moment connection research conducted since the 1994 Northridge Earthquake. Dr. Engelhardt is a member of AISC Task Committee No. Nine on Seismic Design and is a registered Professional Engineer in California.

Summary

The reduced beam section (RBS) moment connection, also known as the "dogbone," is rapidly emerging as a popular choice for seismic-resistant steel moment frames. While research and testing on this connection is continuing, prior research and field experience have shown that the RBS is capable of economically providing ductile and reliable performance.

In the RBS connection, portions of the beam flanges are selectively trimmed in the region adjacent to the beam-to-column connection. A circular radius cutout shape appears to be particularly advantageous. Research has shown that excellent performance can be achieved by combining the RBS cut in the flange together with improved detailing and welding practices at the beam-to-column connection.

This paper will present design recommendations for radius cut RBS moment connections. Previous research on RBS connections is fir briefly reviewed. This is followed by a suggested procedure for sizing the RBS cuts in the beam flanges. Recommendations are than provided on welding and detailing the beam-to-column connection. Finally, a design example is presented to demonstrate the design recommendations.

DESIGN OF REDUCED BEAM SECTION MOMENT CONNECTIONS

INTRODUCTION

Since the 1994 Northridge Earthquake, a variety of new moment connection designs have been developed for seismic resistant steel frames. Among these is the Reduced Beam Section (RBS) moment connection, also known as the dogbone connection. The RBS connection has shown good performance in laboratory testing and is being used on a number of building construction projects. This paper provides preliminary recommendations for the design and detailing of radius cut Reduced Beam Section (RBS) moment connections. Included is a brief description of the RBS moment connection, a description of a suggested design basis for this connection, a procedure for sizing the RBS cut, recommendations on other design and detailing features of the connection, and a design example. An appendix is also included that provides a summary of experimental data for RBS moment connections.

The recommendations provided herein are based on currently available experimental data for RBS connections as interpreted by the writer. Based on this data, it is believed that the radius cut RBS moment connection is capable of developing large levels of plastic rotation under severe cyclic loading on a consistent and reliable basis. However, many issues related to steel moment connections in general, and RBS moment connections in particular are presently the subject of research under the SAC Phase 2 program and under other programs. The reader is encouraged to stay abreast of new research results, as they become available.

BACKGROUND

In an RBS moment connection, also sometimes known as the "dogbone," portions of the beam flange are selectively trimmed in the region adjacent to the beam-to-column connection. Various shapes of cutouts are possible, including a constant cut, a tapered cut, a radius cut and others. Figure 1 illustrates a radius cut RBS connection.

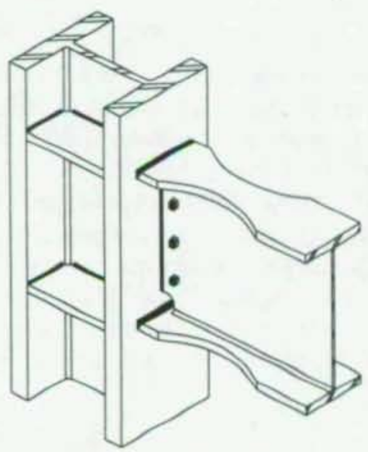

Fig. 1 Radius Cut RBS Moment Connection

The RBS forces yielding and hinge formation to occur within the reduced section of the beam and limits the moment the can be developed at the face of the column. By reducing demands on the beam flange groove welds and the surrounding base metal regions, the RBS reduces the possibility of fractures occurring in this vulnerable region. Although the RBS essentially weakens the beam, its impact on the overall lateral strength and stiffness of a steel moment frame is generally small. Its primary intended effect is to significantly enhance ductility. The RBS plays a role similar to that of connection reinforcement schemes such as cover plates, ribs and haunches. Both the RBS and connection reinforcement move the plastic hinge away from the face of the column and reduce inelastic deformation demands in the vicinity of the beam flange groove welds. Connection reinforcement often requires welds that are difficult and costly to make and inspect. These problems are lessened with the RBS, which is relatively simpler to construct. The smaller moment generated at the face of the column for an RBS connection also offers some advantages in satisfying strong column-weak beam requirements and in minimizing column doubler plate requirements.

A significant amount of research and testing on RBS moment connections has already been completed. Appendix A provides a database of past tests on RBS connections intended for construction of new seismic resistant steel moment frames. This database has been adapted from information provided in Ref. 1. While this database is not exhaustive, it is believed to include the majority of RBS tests conducted as of early 1999. The database includes key features of each test, including member sizes and strengths, connection details, RBS size and shape, and the plastic rotation achieved by each specimen.

Examination of the data in Appendix A reveals that the majority of RBS tests have been quite successful. In most cases, the connections developed at least 3% plastic rotation. A few connections experienced fractures within the RBS or in the vicinity of the beam flange groove welds. Even for these cases, however, the specimens developed on the order of 2% plastic rotation or better. Consequently, the available test data for new construction suggests that the RBS connection can develop large levels of plastic rotation on a consistent and reliable basis. Figure 2 shows an example of a laboratory test of a radius cut RBS specimen (2). The connection detail is shown in Fig. 2(a) and the moment versus plastic rotation response is shown in Fig. 2(b). As is typical of many RBS tests, this specimen showed excellent performance.

As indicated by the data in Appendix A and as shown in Fig. 2(a), it is important to note that most RBS test specimens, in addition to incorporating the RBS, also incorporated significant improvements in welding and in other detailing features as compared to the Pre-Northridge connection. All specimens used welding electrodes that exhibit improved notch toughness as compared to the E70T-4 electrode commonly used prior to the Northridge Earthquake. The majority of specimens also incorporated improved practices with respect to backing bars and weld tabs. In many cases, bottom flange backing bars were removed, and top flange backing bars were seal welded to the column. Further, weld tabs were removed in most cases. In addition to welding related improvements, most specimens also incorporated additional detailing improvements. For example, all specimens employed continuity plates at the beam-to-column connection, although many would not have required them based on UBC requirements in force prior to Northridge Earthquake. A number of specimens also used welded beam web connections rather than the more conventional bolted web. These welded beam web connections were made either by directly welding the web to the column via a complete joint penetration groove weld, or by the use of a heavy welded shear tab. Further, several specimens used reinforcing ribs or cover plates to supplement the RBS. Consequently, although the beam flange cutouts are the most distinguishing feature of the RBS connection, the success of this connection in laboratory tests is also likely related to the many other welding and detailing improvements implemented in the test specimens.

Past experimental work has included successful tests on constant cut, tapered cut and radius cut RBS specimens. The constant cut may offer advantages of simplified fabrication. The tapered cut, on the other hand, is intended to match beam strength to the shape of the moment diagram, thereby promoting more uniform yielding within the reduced section. Both the constant cut and tapered cut RBS connections, however, have experienced fractures within the RBS in some laboratory tests. These fractures have occurred at changes in section within the RBS, for example at the minimum section of the tapered RBS. These changes of cross-section presumably introduce stress concentrations that can lead to fracture within the highly stressed reduced section of the beam. The radius cut RBS appears to minimize stress concentrations, thereby reducing the chances of a fracture occurring within the reduced section. Further, the radius cut is still relatively simple to fabricate. Consequently, the radius cut is recommended for RBS connections. The remainder of this paper is restricted to the design of radius cut RBS connections.

DESIGN BASIS

The following sections contain recommendations for sizing the flange cuts in a radius cut RBS connection as well as recommendations for other design and detailing features of the connection. Many of the design steps parallel recommendations provided in Ref. 1.

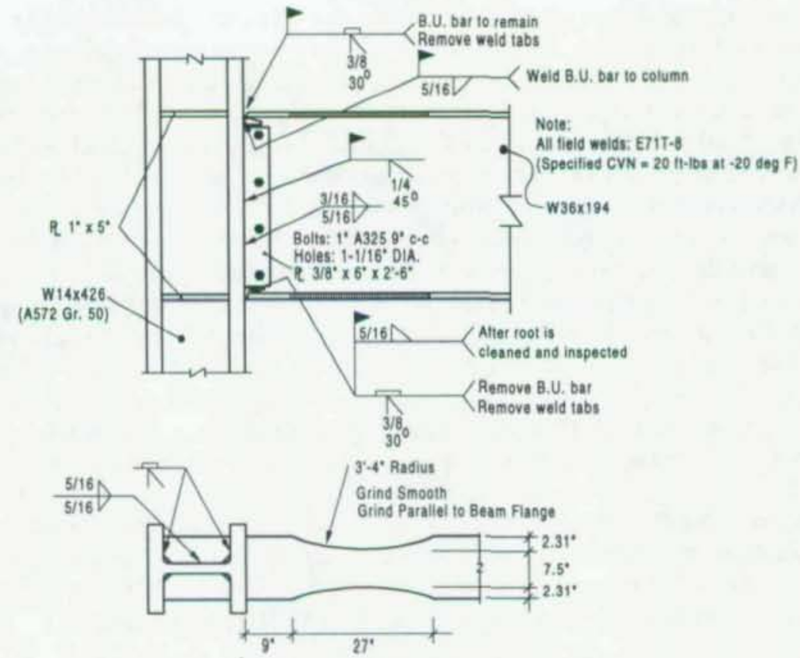

(a) Detail of Test Specimen

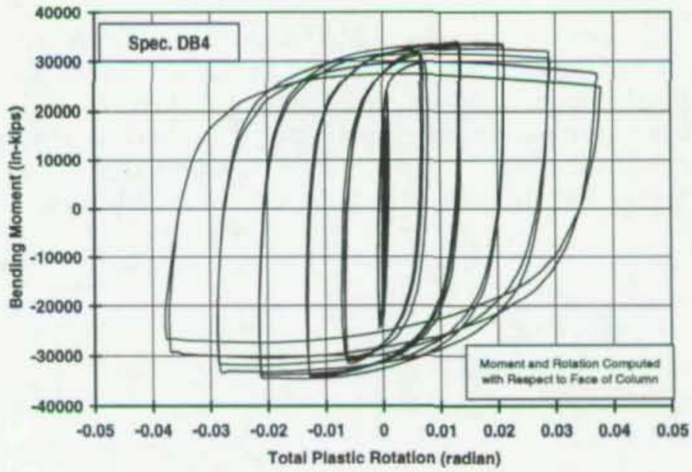

(b) Response of Test Specimen

Fig. 2 Example of Laboratory Behavior of Radius Cut RBS Test Specimen (2)

The overall goal in sizing the RBS cut in the following design procedure is to limit the maximum beam moment that can develop at the face of the column to values in the range of about 85 to 100 percent of the beam's actual plastic moment. This approach, in effect, limits the average stress at the beam flange groove welds to values on the order of the actual yield stress of the beam. Experiments (2) have shown that connections detailed in accordance with the recommendations provided below are capable of safely resisting this level of moment. As a point of comparison, tests on all-welded moment connections without RBS cutouts often show maximum moments at the face of the column of about 125 percent of M_p or greater (7-9). Consequently, the addition of the RBS cutouts in the beam results in a substantial reduction in moment at the face of the column.

Much of the design procedure presented below follows recommendations of the *SAC Interim Guidelines* (4) and the *Interim Guidelines Advisory No. 1* (5), with several exceptions. Most significant of these exceptions is that *Advisory No. 1* places a limit on the maximum stress permitted at the face of the column equal to ninety percent of the minimum specified yield stress of the column. For the normal case of an A572 Gr. 50 column, this results in a limit of 45 ksi. This limit was established to address concerns regarding the potential for through-thickness failures in column flanges. As noted above, the design procedure presented below limits the maximum stress at the face of the column to a value on the order of the actual yield stress of the beam, which may exceed this 45 ksi limit. The actual yield stress of either an A36 or A572 Gr. 50 beam is anticipated to be in the vicinity of approximately 55 ksi (5). This exception to the requirements of *Advisory No. 1* has been adopted for several reasons. First, specimens designed according to the procedures described herein have performed well in laboratory tests. Second, satisfying the 45 ksi stress limit, would in the opinion of the writer, result in excessively large flange cutouts in many cases, or would require supplemental flange reinforcement such as cover plates or ribs. Further, research currently underway under the SAC Phase 2 program suggests that the potential for through-thickness failures is considerably less than previously thought, and that the current limit of 45 ksi can likely be safely increased.

The second area where the design recommendations provided below differ from *Advisory No. 1* is in regard to the need for lateral bracing at the RBS. This issue is discussed in greater detail later.

The design procedure described below assumes that a radius cut RBS is provided in both the top and bottom flanges at the moment connection at each end of a moment frame beam. The procedure also assumes the minimum specified yield stress of the beam is 50 ksi or less (A36 or Gr. 50 beams), and that the minimum specified yield stress of the column is 50 ksi or greater (Gr. 50 or Gr. 65 columns).

PROCEDURE FOR SIZING THE RBS CUT

Figure 3 shows the geometry of a radius cut RBS, and Fig. 4 shows the entire moment frame beam. The key dimensions that must be chosen by the designer are *a*, the distance from the face of the column to the start of the RBS cut, *b*, the length of the RBS cut, and *c*, the depth of the RBS cut at its minimum section. The radius of the cut *R* can be related to dimensions *b* and *c* based on the geometry of a circular arc, using the equation in Fig. 3. The amount of flange material which is removed at the minimum section of the RBS is sometimes referred to the *percent flange removal* which is computed as $(2c/b_f) \times 100$, where b_f is the unreduced flange width of the beam.

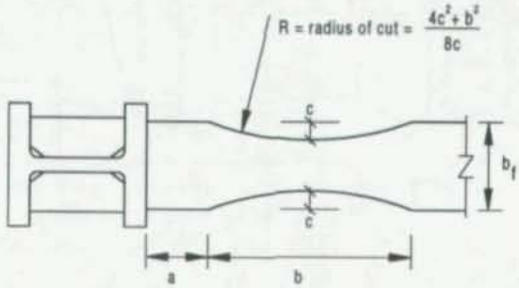

Fig. 3 Geometry of Radius Cut RBS

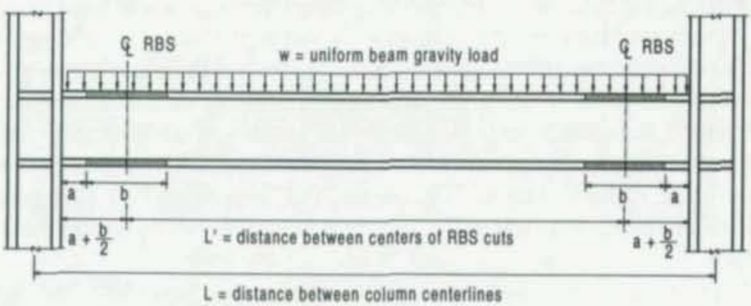

Fig. 4 Typical Moment Frame Beam with RBS Connections

In past tests, the dimensions a and b have generally been chosen based on the judgment of the researchers. In general, these dimensions should be kept as small as possible in order to minimize the growth of moment from the plastic hinge located in the RBS back to the face of the column. The dimension a should be large enough, however, to permit stress in the reduced section of the beam to spread uniformly across the flange width at the face of the column. Similarly, the dimension b should be large enough to avoid excessive inelastic strains within the RBS. Thus, the dimensions a and b should be chosen considering these differing requirements. Based on an evaluation of successful past tests, the following suggestions are made for choosing these dimensions:

$$a \cong (0.5 \text{ to } 0.75)\, b_f \tag{1}$$

$$b \cong (0.65 \text{ to } 0.85)\, d \tag{2}$$

where b_f and d are the beam flange width and depth. Examination of RBS test data indicates that successful connection performance has been obtained for a wide range of values for a and b. Consequently, a great deal of precision in choosing these values does not appear justified and Eqs. 1 and 2 should be considered an approximate guide.

The remaining dimension that must be chosen when sizing the RBS is c, the depth of the cut. The value of c will control the maximum moment developed within the RBS, and therefore will control the maximum moment generated at the face of the column. As noted above, the final dimensions should be chosen so that the maximum moment at the face of the column is in the range of about 85 to 100 percent of the beam's actual plastic moment. At present, the writer suggests avoiding flange reductions greater than about 50 percent. Thus, the value of c should be chosen to be less than or equal to $0.25b_f$.

The remainder of the procedure is presented below in a step-by-step fashion. The basic approach taken in this procedure is to choose preliminary values for a, b and c, then compute the moment at the face of the column, and check this moment against the limit noted above. Some iteration in the RBS dimensions may be needed to arrive upon a satisfactory design.

STEP 1 - Choose trial values for RBS dimensions a, b and c.

The trial values for a and b should be chosen within the limits of Eqs. 1 and 2. To establish a trial value of c, a flange reduction of about 40 percent is suggested for the initial design iteration. Thus, choose $c \cong 0.20\, b_f$. As noted above, values for c in excess of about $0.25b_f$ are not recommended.

STEP 2 - Compute the plastic section modulus at the minimum section of the RBS.

Figure 5 shows a cross-section of the beam at the minimum section of the RBS. Based on the dimensions shown in this figure, Z_{RBS} can be computed as follows:

$$Z_{RBS} = Z_b - 2\,c\,t_f(d - t_f) \tag{3}$$

where:
Z_{RBS} = plastic section modulus at minimum section of RBS
Z_b = plastic section modulus for full beam cross-section (i.e. without flange cutouts)
other variables as shown in Fig. 5.

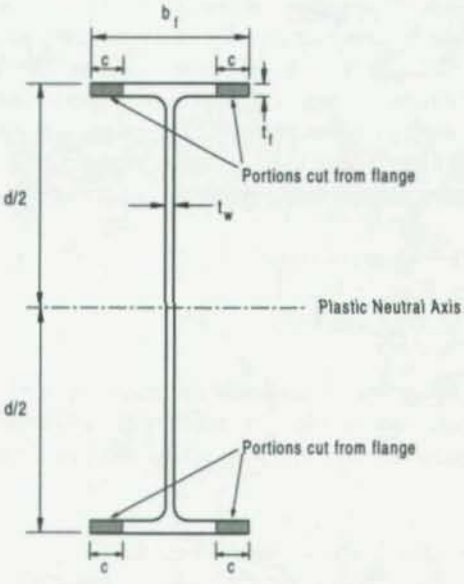

Fig. 5 Beam at Minimum Section of RBS

STEP 3 - Establish the expected yield stress of the beam.

The expected yield stress for the beam can be determined from Section 6.2 of the AISC *Seismic Provisions for Structural Steel Buildings* (6). According to these provisions:

$$F_{ye} = R_y F_y \tag{4}$$

where:

F_{ye} = expected yield stress
F_y = minimum specified yield stress
R_y = ratio of expected to minimum specified yield stress
= 1.5 for A36 steel
= 1.1 for A572 Gr. 50 steel

The value of F_{ye} recognizes that the actual yield strength of structural steel can be significantly in excess of its minimum specified value.

STEP 4 - Compute the maximum moment expected at the center of the RBS.

$$M_{RBS} = 1.15\, Z_{RBS}\, F_{ye} \tag{5}$$

where:

M_{RBS} = maximum moment expected at the center of the RBS
Z_{RBS} = plastic section modulus at minimum section of the RBS
F_{ye} = expected yield stress of beam

The factor of 1.15 in Eq. 5 accounts for strain hardening, and is based on measured strain hardening values reported in Ref. 2.

STEP 5 - Compute the shear force at the center of the RBS cuts at each end of the beam.

The shear at the center of the RBS cuts can be computed from a free body diagram of the moment frame beam taken between RBS centers. Such a free body diagram is illustrated in Fig. 6 for the case of a uniformly distributed gravity load *w*.

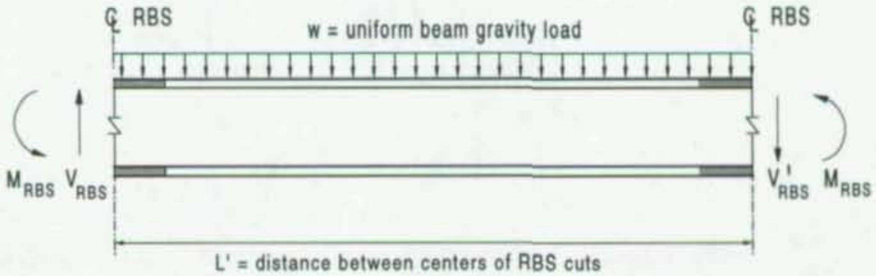

Fig. 6 Free Body Diagram Between RBS Cuts

Summing moments about each end of this free body diagram results in the following:

$$V_{RBS} = \frac{2M_{RBS}}{L'} + \frac{wL'}{2} \tag{6a}$$

$$V'_{RBS} = \frac{2M_{RBS}}{L'} - \frac{wL'}{2} \tag{6b}$$

where:

V_{RBS} ,V'_{RBS}	=	shear force at the center of the RBS cuts at each end of beam (V_{RBS} is the larger shear force, V'_{RBS} is the smaller shear force)
L'	=	distance between centers of RBS cuts
w	=	uniformly distributed gravity load on beam

For gravity load conditions other than a uniform load, the appropriate adjustment can easily be made to the free body diagram and to Eqs. 6a and 6b.

Eqs. 6a and 6b assume that plastic hinges will form at the RBS at each end of the beam. If the gravity load on the beam is very large, the plastic hinge at one end of the beam may move towards the interior portion of the beam span. If this is the case, the free body diagram in Fig. 6 should be modified to extend between the actual plastic hinge locations. To check if Eqs. 6a and 6b are valid, draw the moment diagram for the segment of the beam shown in Fig. 6, i.e., for the segment of the beam between the centers of the RBS cuts. If the maximum moment occurs at the ends of the spans, then Eqs. 6a and 6b are valid. If the maximum moment occurs within the span, and exceeds M_{pe} of the beam (see Eq. 8), then the modification described above will be needed.

<u>STEP 6</u> - Compute the maximum moment expected at the face of the column.

The moment at the face of the column can be computed from a free body diagram of the segment of the beam between the center of the RBS and the face of the column. Such a free body diagram is illustrated in Fig. 7.

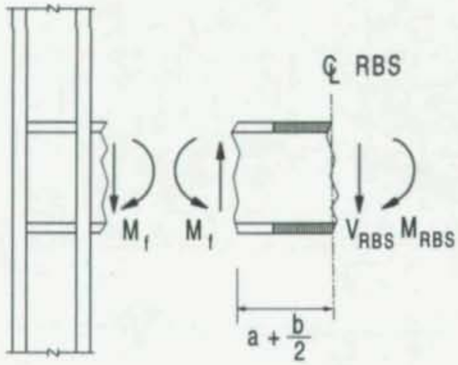

Fig. 7 Free Body Diagram Between Center of RBS and Face of Column

Summing moments for this free body diagram results in the following:

$$M_f = M_{RBS} + V_{RBS}\left(a + \frac{b}{2}\right) \tag{7}$$

where:

M_f = maximum moment expected at the face of the column

Eq. 7 neglects the gravity load on the portion of the beam between the center of the RBS and the face of the column. This simplifies the equation and introduces little error. If desired, the gravity load on this small portion of the beam can be included in the free body diagram and in Eq. 7.

STEP 7 - Compute the plastic moment of the beam based on the expected yield stress.

$$M_{pe} = Z_b \, F_{ye} \tag{8}$$

where:

M_{pe} = plastic moment of beam based on expected yield stress.

STEP 8 - Check that M_f is in the range of 85 to 100 percent of M_{pe}.

$$\frac{M_f}{M_{pe}} \equiv 0.85 \ to \ 1.0 \tag{9}$$

If Eq. 9 is not satisfied, increase the value of c, and/or decrease the values of a and b, and repeat Steps 2 through 8.

ADDITIONAL DESIGN AND DETAILING CONSIDERATIONS

In addition to establishing the dimensions of the RBS cut, there are a number of additional design and detailing features that may significantly affect connection performance and economy. These items are discussed below.

Fabrication of RBS Cuts

The procedure presented above for sizing the RBS cut permits a range of acceptable values for the dimensions a, b and c. Fabrication can likely be simplified by standardizing these dimensions over a large number of beams on a project. Making small changes on the RBS dimensions from beam to beam is not likely to improve connection performance and may unnecessarily increase fabrication costs. The designer may wish to consult with a fabricator before finalizing the RBS dimensions to identify ways of reducing fabrication costs. For example, if the fabricator is making RBS cuts using a torch mounted on a guide with a fixed radius, the economy of the connection may be improved by maintaining a constant radius of cut *R* over a large number of connections.

The RBS cut is normally made by thermal cutting. The cut should be as smooth as possible, avoiding nicks, gouges, and other discontinuities. After the cut is made, the surface should be ground smooth, with the grinding done in a direction parallel to the beam flange. This avoids grind marks perpendicular to the beam flange, i.e., perpendicular to the direction of stress, which can act as stress risers.

Welding Considerations

Research conducted since the Northridge Earthquake has demonstrated the importance of weld metal toughness in the groove welds of seismic resistant moment connections (11,12). The minimum toughness needed for groove welds in this application has not yet been quantified. However, a number of successful tests have employed E70 electrodes with a minimum specified Charpy V-Notch (CVN) value of 20 ft.-lb. at -20° F. Thus, pending further research and based on available test data on RBS connections, it is recommended that weld metal for groove welds be specified to provide a minimum specified tensile strength of 70 ksi, and a minimum specified CVN value of 20 ft.-lb. at -20° F. Past tests on RBS connections have generally employed the self shielded flux cored arc welding process (FCAW), using either the E70TG-K2, E71T-8 or the E70T-6 electrodes, all of which provide a minimum specified CVN of 20 ft.-lb. at -20° F. The final choice of welding process and electrode is best left to the fabricator.

At the beam flange groove welds, it is recommended that the weld tabs be removed at both the top and bottom flanges, and the edges of the groove welds ground smooth. This will minimize any potential notches introduced by the presence of the weld tabs, or by discontinuities contained in the weld metal within the run-off regions. In addition, it is recommended that the bottom flange steel backing be removed and a reinforcing fillet be placed at the base of the groove weld. This requirement is intended to eliminate the notch effect produced by left-in-place steel backing, and to permit better inspection and ultrasonic testing of the weld. At the top flange groove weld, it is recommended that the steel backing be seal welded to the face of the column using a minimum size fillet weld, typically a 5/16″ fillet. Analysis has indicated that the notch effect of the steel backing is not as severe at the top flange, and that welding the steel backing to the column further reduces the notch effect. Further, defects are less likely at the top flange weld since neither the groove weld nor the ultrasonic testing of the groove weld is interrupted by the beam web, as they are at the bottom flange.

The size, shape and finish of the weld access holes can also have an important effect on the performance of the connection. Although current research is addressing issues related to the weld access hole, there appears to be no consensus as of yet on the optimum size and shape. Consequently, pending further research, access hole geometry should conform to the requirements shown in Figure 5.2 of AWS D1.1-98 (13). The point where the access hole meets the inside face of the flange is a potential fracture initiation site. Consequently, a smooth transition between the access hole and the inside face of the beam flange appears particularly important.

All welding should be specified to be in conformance with AWS D1.1-98. Acceptance criteria for ultrasonic testing of groove welds is recommended to be in conformance with Table 6.2 of AWS D1.1-98. Additional useful information on welding moment connections can be found in a number of references, including Refs. 4,5,17 and 18.

Beam Web Connection

It is recommended that the connection of the beam web to the column be welded. While a welded web connection is more costly than the more conventional bolted web connection, it is believed that the welded web improves the reliability of the connection. The welded web provides for more effective force transfer through the web connection, thereby reducing demands at the beam flanges and beam flange groove welds. Past tests have suggested better connection performance is possible with a welded web (7-9).

The welded web connection can be made by specifying a complete joint penetration (CJP) groove weld between the beam web and column flange over the full depth of the web. An example is shown in Fig. 2. Normally, a shear tab, which is welded to the column and bolted to the beam web, is still provided. This shear tab serves several purposes. First, it acts as backing for the CJP groove weld. Secondly, it carries erection loads and helps maintain the frame in a plumb position until welding at the connection is completed. Since the shear tab is provided for erection purposes only, it is recommended that the design of the shear tab be left to the fabricator.

As an alternative to a CJP groove weld, the beam web connection can also be made using a heavy welded shear tab. The shear tab is typically welded to the column using either fillet welds or a CJP groove weld. The shear tab, in turn, is then welded to the beam web with fillet welds. An example of such a connection can be found in Ref. 10.

Continuity Plates

All of the successful tests on RBS connections for new construction (Appendix A) have employed continuity plates. However, no RBS tests have omitted continuity plates, so it is unclear under what conditions continuity plates are actually required. Pending the outcome of further research, it is recommended that continuity plates be provided for all RBS connections, with a continuity plate thickness similar to the beam flange thickness. When CJP groove welds are used for attaching a continuity plate to the column flange or web, use of an electrode with a rated CVN of at least 20 ft.-lb. at -20° F is suggested. Removal of backing bars from continuity plate welds, however, does not appear necessary. When welding the continuity plates to the column, welding in the "k-region" of the column should be avoided. Further information on potential problems in this area can be found in Refs. 6 and 14.

Supplemental Lateral Bracing at RBS

SAC *Advisory No. 1* recommends that a lateral brace be provided at the RBS. This recommendation addresses the concern that a beam with RBS cuts may be prone to earlier or more severe instability than a beam without RBS cuts.

Virtually all moment connections that dissipate energy by yielding of the beam are subject to varying degrees of beam instability at large levels of inelastic rotation. This is true both for reinforced connections (cover plates, ribs, haunches, etc.) and for RBS connections. This instability generally involves a combination of flange buckling, web buckling and lateral torsional buckling and typically results in a deterioration in the flexural strength of the beam with increasing inelastic rotations. In the experience of the writer, the degree of instability and associated strength deterioration for RBS connections tested in the laboratory have been no more severe, and perhaps somewhat less severe than for many types of reinforced connections. This is demonstrated by the connection test results shown in Fig. 8.

This figure shows a plot of beam tip load versus beam tip displacement for two different test specimens (Refs. 2 and 15). These two specimens were virtually identical, except for the connection detail. Both specimens were constructed with the same member sizes (W36x150 beam and W14x426 column) and heats of steel, and tested in the same test setup with identical member lengths, identical member end support conditions, and identical lateral bracing. Both specimens were subject to the same loading history. The only difference was that one specimen was constructed with a cover plated connection and the other with an RBS connection. Both specimens were provided with a single beam lateral support near the point of load application.

As can be seen from Fig. 8, the peak strength of the RBS connection is less than that of the cover plated connection. This, of course, is expected and is in fact the advantage of the RBS in that it reduces the moment generated at the connection and the moment delivered to the column. After reaching their peak strength, both connections exhibited some strength deterioration due to combined flange, web and lateral torsional buckling in the beam. Note however that the rate of deterioration is less for the RBS specimen. In fact, at large inelastic deformations, the RBS exhibits the same strength as the cover plated connection. This comparison demonstrates the observation made above, i.e., RBS connections exhibit no more strength deterioration, and perhaps somewhat less deterioration than reinforced connections.

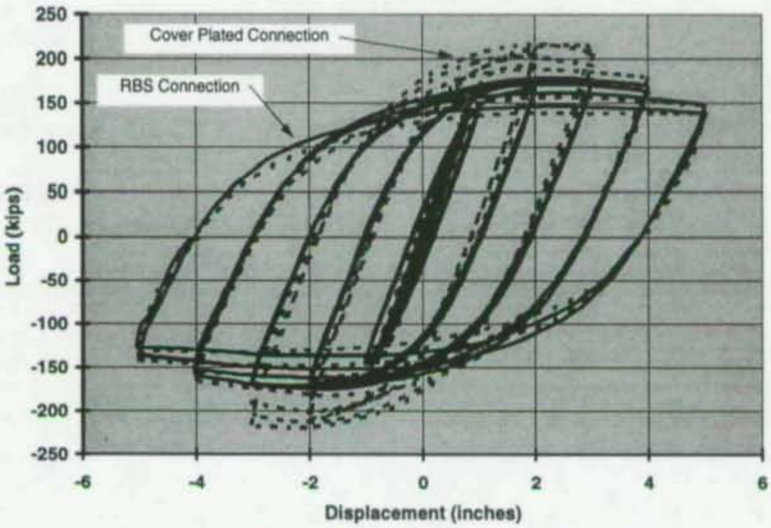

Fig. 8 - Comparison of Test Results for Cover Plated and RBS Connections

The test data summarized in Appendix A indicates that many RBS connection tests have been conducted without an additional lateral brace at the RBS, without reports of unusually severe or unacceptable strength deterioration due to the absence of a lateral support.

Based on the available experimental data, in the judgment of the writer, no additional lateral support is required at the RBS. Of course, the designer should still adhere to the normal code provisions for beam lateral support and for beam flange and web slenderness limits (6).

Checking Code Strength and Drift Requirements

After sizing the RBS cuts, it is also necessary to check that the resulting frame satisfies all appropriate code requirements for strength and stiffness. The strength of the beam at the minimum section of the RBS must satisfy code requirements under all applicable load combinations including gravity, wind, and any other loads appropriate for the structure under consideration. Beam sizes in typical moment frames are normally governed by code specified drift limits. Consequently, even with a reduction in beam strength due to the addition of the RBS, the strength of the modified frame will often be satisfactory for all load combinations. In some cases, an increase in beam size may be needed.

The addition of RBS cutouts will reduce the stiffness of a steel moment frame. This reduction in stiffness, although generally quite small, may affect the ability of the frame to satisfy code specified drift limits. A recent study Grubbs (16) evaluated the reduction in elastic lateral stiffness of steel moment frames due to the addition of radius cut RBS connections. This study showed that over a wide range of frame heights and configurations, the average reduction in stiffness for a 50 percent flange reduction was on the order of 6 to 7 percent. For a 40 percent flange reduction, the reduction in elastic frame stiffness was on the order of 4 to 5 percent. If this reduction in stiffness is a concern, drift can be computed in the usual manner using a model that does not explicitly account for the RBS, and then increased by the amounts noted above to account for the RBS connections. Alternatively, a refined structural model including the RBS cuts can be developed to check the stiffness of the frame.

DESIGN EXAMPLE

Description of Frame

Frame centerline dimensions: story height = 12′ - 0″
bay width = 30′ - 0″

Beam:	W36x150	A572 Gr. 50 with special requirements per AISC Technical Bulletin No. 3, dated March 1997
Column:	W14x426	A572 Gr. 50 with special requirements per AISC Technical Bulletin No. 3, dated March 1997

Gravity load on beam, based on 1.2D + .5L per Sect. 9.2c of Ref. 6: 3 kips/ft (0.25 kips/in)

Design typical interior moment connection.

Section Properties:

W36x150: $d = 35.85''$
$b_f = 11.975''$
$t_f = .94''$
$t_w = .625''$
$Z = 581 \text{ in}^3$

W14x426: $d = 18.67''$
$b_f = 16.695''$
$t_f = 3.035''$
$t_w = 1.875''$
$Z = 869 \text{ in}^3$

1. Choose trial values for RBS dimensions *a*, *b* and *c*

$a \cong (0.5 \text{ to } 0.75)\, b_f = 6'' \text{ to } 9''$ Try: $a = 7''$
$b \cong (0.65 \text{ to } 0.85)\, d = 23'' \text{ to } 30''$ Try: $b = 25''$
$c \cong 0.2\, b_f = 2.4''$ Try: $c = 2.5''$

2. Compute the plastic section modulus at the minimum section of the RBS

From Eq. 3:

$$Z_{RBS} = Z_b - 2\,c\,t_f\,(d - t_f) = 581 - 2 \times 2.5 \times 0.94 \times (35.85 - 0.94) = 417 \text{ in}^3$$

3. Establish the expected yield stress of the beam

For A572 Gr. 50 steel, $R_y = 1.1$. From Eq. 4:

00290

$$F_{ye} = R_y F_y = 1.1 \times 50 = 55 \text{ ksi}$$

4. Compute the maximum moment expected at the center of the RBS

From Eq. 5:

$$M_{RBS} = 1.15\, Z_{RBS}\, F_{ye} = 1.15 \times 417 \times 55 = 26375 \text{ kip-in.}$$

5. Compute the shear force at the center of the RBS cuts at each end of the beam

$$L' = L - d_c - 2\left(a + \frac{b}{2}\right) = 360 - 18.7 - 2\left(7 + \frac{25}{2}\right) = 302''$$

From Eqs. 6a and 6b:

$$V_{RBS} = \frac{2\ M_{RBS}}{L'} + \frac{wL'}{2} = \frac{2 \times 26375}{302} + \frac{0.25 \times 302}{2} = 212 \text{ kips}$$

$$V'_{RBS} = \frac{2\ M_{RBS}}{L'} - \frac{wL'}{2} = \frac{2 \times 26375}{302} - \frac{0.25 \times 302}{2} = 137 \text{ kips}$$

Figure 8 shows the free body diagram, the shear force diagram and the bending moment diagram for the portion of the beam between RBS centers. Observe that the maximum moment occurs at the ends, i.e., at the centers of the RBS cuts. This indicates that the gravity load is not so large that a plastic hinge will form within the span away from the RBS. Consequently, the calculations above for the moment and shear forces at the RBS cuts are valid.

6. Compute the maximum moment expected at the face of the column

From Eq. 7:

$$M_f = M_{RBS} + V_{RBS}\left(a + \frac{b}{2}\right) = 26375 + 212\left(7 + \frac{25}{2}\right) = 30510 \text{ kip-in}$$

7. Compute the plastic moment of the beam based on the expected yield stress

From. Eq. 8:

$$M_{pe} = Z_b\, F_{ye} = 581 \times 55 = 31955 \text{ kip-in}$$

8. Check that M_f is in the range of 85 to 100 percent of M_{pe}

From Eq. 9:

$$\frac{M_f}{M_{pe}} = \frac{30510}{31955} = 0.96 \qquad \underline{\underline{OK}}$$

Thus, the preliminary dimensions are OK. Use: $a = 7''$, $b = 25''$, $c = 2.5''$, $R = 32.5''$.

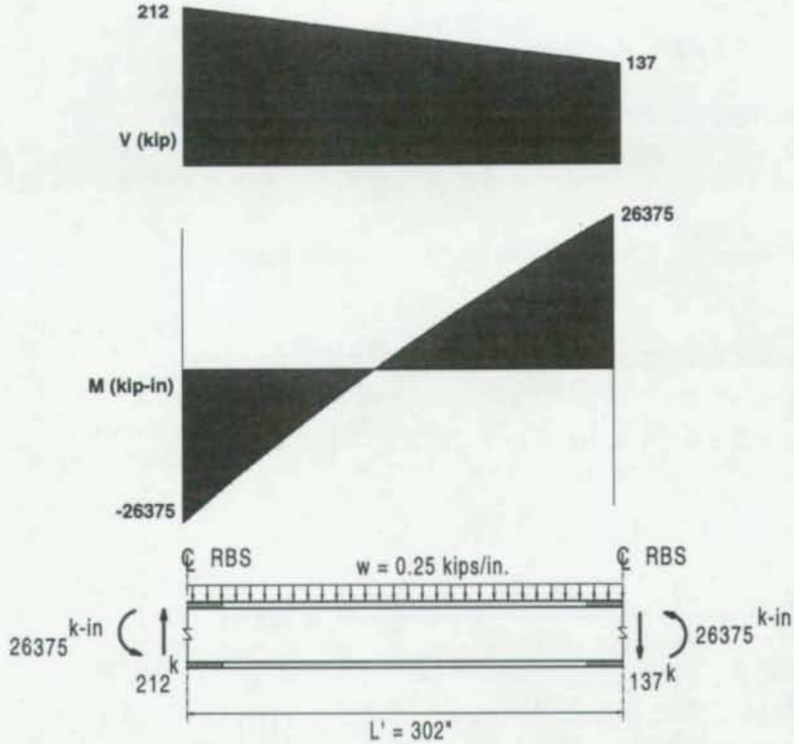

Fig. 8 Portion of Example Beam Between RBS Centers

Additional Design Issues

In the remainder of the example, additional design issues will be considered, including strong column-weak beam check, column panel zone check, continuity plate design, and beam web connection design.

Strong Column - Weak Beam Check

To check strong column-weak beam requirements, the procedure presented in the *SAC Advisory No. 1* (5) will be used, with minor modification. The equation to be used to check this requirement (from Eq. 7.5.2.5-1-4 of *Advisory No. 1)* is as follows:

$$\frac{\sum Z_c\left(F_{yc} - f_a\right)}{\sum M_c} > 1.0 \tag{10}$$

where:

Z_c = plastic section modulus of the column section above and below the connection

F_{yc} = minimum specified yield stress of the column

f_a = axial stress in the column above and below the connection

ΣM_c = sum of the column moments at the top and bottom of the panel zone corresponding to the development of M_{RBS} at the center of the RBS cuts in the attached beams

Figure 9 shows a free body diagram that can be used to estimate column moments when checking Eq. 10. This free body cuts the beams at the RBS centers and cuts the columns at assumed points of inflection.

Based on Fig. 9, ΣM_c can be estimated from the following equations:

$$V_c = \frac{\sum M_{RBS} + \left(V_{RBS} + V'_{RBS}\right)\left(\frac{d_c}{2} + a + \frac{b}{2}\right)}{h_t + d_b + h_b} \tag{11}$$

$$M_{ct} = V_c h_t \tag{12}$$

$$M_{cb} = V_c h_b \tag{13}$$

$$\sum M_c = M_{ct} + M_{cb} \tag{14}$$

where:

V_c = shear force in the columns above and below the connection
M_{ct} = column moment immediately above connection
M_{cb} = column moment immediately below connection
h_t = distance from top of beam to point of inflection in the column above the connection
h_b = distance from bottom of beam to point of inflection in the column below the connection
d_b = depth of beam

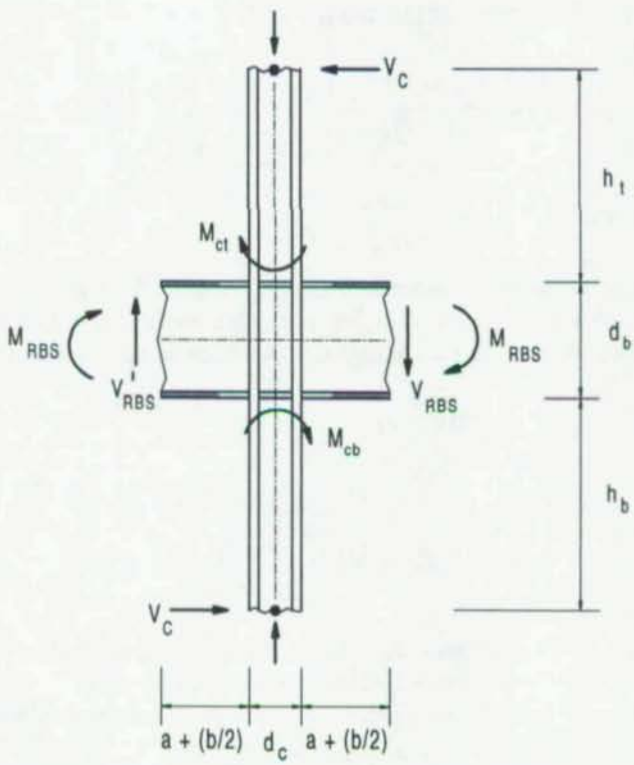

Fig. 9 Free Body Diagram for Calculation of Column Moments

The above approach is a simplified version of the approach presented in *SAC Advisory No. 1*. *Advisory No. 1* accounts for the difference in column shear forces above and below the connection, whereas the simplified approach above assumes the same shear force is present in the columns above and below the connection. Although the approach in *Advisory No. 1* may be somewhat more accurate, the computation of V_c presented in Eq. 11 above is simpler to implement, and is still reasonably accurate for design purposes considering the numerous uncertainties involved in the strong column-weak beam design philosophy. The reader is referred to Section 7.5.2.5 of *Advisory No. 1* should they desire to implement a more accurate calculation for V_c.

Returning to the example, assuming that points of inflection in the columns occur at their hid-heights, and assuming an axial stress of 15 ksi in the columns under combined earthquake and gravity loading, the following calculations result.

$$V_c = \frac{\sum M_{RBS} + \left(V_{RBS} + V'_{RBS}\right)\left(\frac{d_c}{2} + a + \frac{b}{2}\right)}{h_t + d_b + h_b}$$

$$= \frac{2 \times 26375 + (212 + 137)\left(\frac{18.7}{2} + 7 + \frac{25}{2}\right)}{144} = 436 \text{ kips}$$

$M_{ct} = V_c\, h_t = 436 \times (144 - 35.85)/2 = 23575$ kip-in

$M_{cb} = 23575$ kip-in

$\sum M_c = 2 \times 23575 = 47150$ kip–in

$$\frac{\sum Z_c\left(F_{yc} - f_a\right)}{\sum M_c} = \frac{2 \times 869(50 - 15)}{47150} = 1.3 > 1 \quad \underline{\underline{OK}}$$

Check Column Panel Zone

To check the column panel zone, the procedure used in Section 7.5.2.6 of *SAC Advisory No. 1* will be used. This section requires that the panel zone has sufficient strength to develop the shear force developed by $0.8\, \Sigma\, M_f$. Based on this approach, the panel zone shear force can be computed as follows:

$$V_{PZ} = \frac{0.8 \sum M_f}{0.95\, d_b} - 0.8 V_c \tag{15}$$

$$\Sigma M_f = M_f + M'_f \tag{16}$$

$$M'_f = M_{RBS} + V'_{RBS}\left(a + \frac{b}{2}\right) \tag{17}$$

where:

V_{PZ} = panel zone shear force corresponding to the development of 80 percent of the maximum expected column face moments

M_f = maximum moment expected at the face of the column, calculated according to Eq. 7

M'_f = maximum moment expected at opposite column face

The value of M_f computed according to Eq. 7 combines the seismic moment due to $(2 \times M_{RBS})/L'$ with the moment due to gravity load. On the side of the column opposite to that where M_f is developed, the moment at the face of the column will be somewhat smaller since the gravity load moment will oppose the seismic moment. This somewhat smaller moment is calculated using Eq. 17.

Returning to the example, the column panel zone shear is computed as follows:

$M_f = 30510$ kip-in

$$M'_f = M_{RBS} + V'_{RBS}\left(a + \frac{b}{2}\right) = 26375 + 137\left(7 + \frac{25}{2}\right) = 29045 \text{ kip-in}$$

$\Sigma M_f = M_f + M'_f = 30510 + 29045 = 59555$ kip-in

$$V_{PZ} = \frac{0.8\sum M_f}{0.95\, d_b} - 0.8V_c = \frac{0.8 \times 59555}{0.95 \times 35.85} - 0.8 \times 436 = 1050 \text{ kips}$$

The strength of the panel zone is calculated as follows per Section 7.5.2.6 of *SAC Advisory No. 1:*

$$V = 0.55F_{yc}d_c t\left[1 + \frac{3b_c t_{cf}^2}{d_b d_c t}\right] \tag{18}$$

where:

V = panel zone shear strength
b_c = width of column flange
t_{cf} = thickness of column flange
t = total thickness of panel zone including doubler plates

For the example, panel zone strength is computed as follows:

$$V = 0.55F_{yc}d_c t\left[1 + \frac{3b_c t_{cf}^2}{d_b d_c t}\right]$$
$$= 0.55 \times 50 \times 18.67 \times 1.875\left[1 + \frac{3 \times 16.7 \times (3.035)^2}{35.85 \times 18.67 \times 1.875}\right] = 1315 \text{ kips}$$

$1315 > 1050$ $\therefore$ No doubler plates required

Continuity Plates

Use continuity plates with a thickness approximately equal to the beam flange thickness. The beam flange thickness is 0.94 inches. Therefore, use one inch thick continuity plates. Connect continuity plates to column flanges and web using CJP groove welds. Snip corners of continuity plates to avoid welding into the k-area of the column.

Beam Web Connection

Connect beam web to column flange using CJP groove weld over full depth of web (between weld access holes).

A drawing of the final connection detail is shown in Fig. 10. The resulting frame should be checked for all code specified strength and drift limits. Note that the RBS flange reduction is approximately 42 percent. Consequently, it is expected that the inclusion of the RBS cuts in the beams will increase interstory drift by about 5 percent.

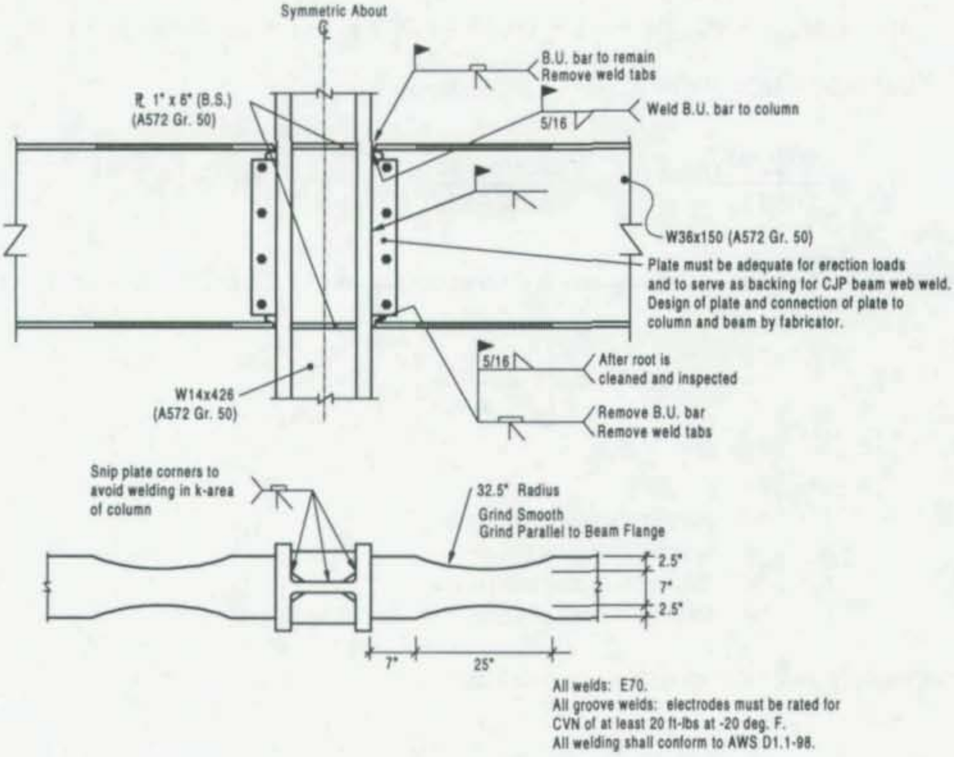

Fig. 10 Connection Detail for Design Example

CONCLUSIONS

The Reduced Beam Section is rapidly emerging as a popular choice for moment resisting connections in seismic resistant steel moment frames. Past research has demonstrated that good connection performance is possible by combining radius cuts in the beam flanges with appropriate detailing and welding at the beam-to-column connection. This paper has provided design and detailing suggestions for radius cut RBS connections based on presently available research. However, research and testing on RBS moment connections is continuing at a rapid pace. Consequently, the reader is encouraged to stay informed of new research results as they become available.

ACKNOWLEDGEMENTS

The writer gratefully acknowledges financial and in-kind support for research on RBS connections from the following organizations: the American Institute of Steel Construction, W&W Steel Company, the National Science Foundation (Grant Nos. CMS-9358186 and CMS-9416287), the National Institute of Standards and Technology (Award No. 70NANB5H0128), the SAC Joint Venture, and the Structural Shape Producers Council. Special thanks are due to Ted Winneberger of W&W Steel Company for suggesting the radius cut RBS and for his continued support and encouragement of RBS research. Thanks are also due to Dr. John Gross of NIST for assistance in developing the design approach and procedure. The writer also thanks Prof. Gary Fry of Texas A&M University for many useful contributions and ideas developed in the course of on-going research on RBS connections. The writer also thanks Bob Pyle of AISC Marketing for his encouragement in the development this paper. The opinions expressed in this paper are those of the writer, and do not necessarily reflect the views of the sponsors or of the individuals just noted.

00293

REFERENCES

1. Gross, J.L., Engelhardt, M.D., Uang, C.M., Kasai, K. and Iwankiw, N., "Modification of Existing Welded Steel Moment Frame Connections for Seismic Behavior," National Institute of Standards and Technology and the American Institute of Steel Construction, Inc. (to be published as AISC Design Guide in late 1998).
2. Engelhardt, M.D., Winneberger, T., Zekany, A.J. ,and Potyraj, T., "Experimental Investigation of Dogbone Moment Connections," *Engineering Journal,* American Institute of Steel Construction , Vol. 35, No. 4, Fourth Quarter 1998.
3. Engelhardt, M.D., Winneberger, T., Zekany, A.J. ,and Potyraj, T., "The Dogbone Connection: Part II." *Modern Steel Construction,* August 1996.
4. SAC Joint Venture, "Interim Guidelines: Evaluation, Repair, Modification and Design of Welded Steel Moment Frame Structures," Published by the Federal Emergency Management Agency, *Report FEMA 267*, August 1995.
5. SAC Joint Venture, "Interim Guidelines Advisory No. 1 - Supplement to FEMA 267," Published by the Federal Emergency Management Agency, *Report FEMA 267A*, March 1997.
6. "Seismic Provisions for Structural Steel Buildings," American Institute of Steel Construction, Inc., Chicago, April 15, 1997.
7. Popov, E. and Stephen, R., " Cyclic Loading of Full Size Steel Connections, " Bulletin No. 21, American Iron and Steel Institute, 1972.
8. Tsai, K.C. and Popov, E.P., "Steel Beam-Column Joints In Seismic Moment Resisting Frames", *Report No. UCB/EERC - 88/19*, Earthquake Engineering Research Center, University of California at Berkeley, 1988.
9. Engelhardt, M.D. and Husain, A.S., "Cyclic Loading Performance Of Welded Flange - Bolted Web Connections," *Journal of Structural Engineering,* ASCE, Vol. 119, No. 12, December 1993.
10. Zekioglu, A., Mozaffarian, H. and Uang, C., "Moment Frame Connection Development and Testing for the City of Hope National Medical Center," *Proceedings; Structures Congress XV,* Portland, April 13-16, 1997, American Society of Civil Engineers, 1997.
11. Kaufmann, E., Xue, M., Lu, L., and Fisher, J., "Achieving Ductile Behavior of Moment Connections," *Modern Steel Construction*, Vol. 36, No. 1, American Institute of Steel Construction, January 1996.
12. Tide, R., "Stability of Weld Metal Subjected to Cyclic Static and Seismic Loading," *Engineering Structures*, Vol. 20, Nos. 4-6, April-June 1998.
13. "Structural Welding Code - Steel," *AWS D1.1-98*, American Welding Society, Miami, 1998.
14. "AISC Initiates Research Into k Area Cracking," *Modern Steel Construction*, Vol. 37, No. 9, September 1997, pp.23-24.
15. Engelhardt, M.D. and Sabol, T.A., "Reinforcing of Steel Moment Connections with Cover Plates: Benefits and Limitations," *Engineering Structures*, Vol. 20, No. 6, pp. 510-520, 1998.
16. Grubbs, K.V., "The Effect of the Dogbone Connection on the Elastic Stiffness of Steel Moment Frames," M.S. Thesis, Department of Civil Engineering, The University of Texas at Austin, Austin, Texas, August 1997.
17. Blodgett, O., Funderburk, S., and Miller, D., "Fabricators' and Erectors' Guide to Welded Steel Construction," The Lincoln Electric Company, Cleveland, 1997.
18. SAC Joint Venture, "Background Reports on Metallurgy, Fracture Mechanics, Welding, Moment Connections and Frame Systems Behavior," Published by the Federal Emergency Management Agency, *Report FEMA 288*, 1996.
19. Chen, S.J., Yeh, C.H. and Chu, J.M, "Ductile Steel Beam-to-Column Connections for Seismic Resistance," *Journal of Structural Engineering*, Vol. 122, No. 11, November 1996, pp. 1292-1299.
20. Iwankiw, N.R., and Carter, C., "The Dogbone: A New Idea to Chew On," *Modern Steel Construction*, April 1996.
21. Zekioglu, A., Mozaffarian, H., Chang, K.L., Uang, C.M. and Noel, S., "Designing After Northridge," *Modern Steel Construction,* March 1997.
22. Popov, E.P., Yang, T.S. and Chang, S.P., "Design of Steel MRF Connections Before and After 1994 Northridge Earthquake," *International Conference on Advances in Steel Structures,* Hong Kong, December 11-14, 1996. Also in: *Engineering Structures,* 20(12), 1030-1038, 1998.

23. Tremblay, R., Tchebotarev, N. and Filiatrault, A., "Seismic Performance of RBS Connections for Steel Moment Resisting Frames: Influence of Loading Rate and Floor Slab," *Proceedings, Stessa '97*, August 4-7, 1997, Kyoto, Japan.
24. Plumier, A., "New Idea for Safe Structures in Seismic Zones," *IABSE Symposium - Mixed Structures Including New Materials*, Brussels, 1990.
25. Plumier, A., "The Dogbone: Back to the Future," *Engineering Journal*, American Institute of Steel Construction, Inc. 2nd Quarter 1997.
26. Uang, C.M., *Unpublished preliminary test reports on SAC Phase 2 RBS tests*, University of California at San Diego, December 1998.

APPENDIX A

SUMMARY OF EXPERIMENTS ON REDUCED BEAM SECTION MOMENT CONNECTIONS FOR NEW CONSTRUCTION

(Adapted from Ref. 1)

Ref	Spec.	Beam	Column	Flange Welds	Web Connection	RBS Details and Other Flange Modifications	θ_p (%)	Comments
[19]	YC-1	Built-up W shape d=23.6", b_f=11.8", t_f=0.79", t_w=0.47" L_b=73" A36 steel F_{y-f}=40 ksi F_{u-f}=66 ksi F_{y-w}=40 ksi F_{u-w}=65 ksi	Built-up Box: 19.7"x19.7"x.79" L_c = 87" A572 Gr. 50 F_y=56 ksi F_u=82 ksi	SS-FCAW E70T-7 No weld tabs used	Bolted: 7-7/8" A325	Tapered cut L_1=2" L_{RBS}=13.8" FR=20%	2.4	Fracture of beam flange initiating at weld access hole
[19]	YC-2	"	"	"	"	Tapered cut L_1=2" L_{RBS}=17.7" FR=25%	2.9	Fracture of beam flange initiating at weld access hole
[19]	PC-1	"	"	"	"	Tapered cut L_1=4.7" L_{RBS}=15.7" FR=34%	4.1	Fracture of beam flange initiating at weld access hole
[19]	PC-2	"	"	"	"	Tapered cut L_1=4.7" L_{RBS}=17.7" FR=42%	4.8	Fracture of beam flange initiating at weld access hole
[19]	PC-3	"	"	"	"	Tapered cut L_1=4.7" L_{RBS}=17.7" FR=42%	3.8	Fracture of beam flange initiating at weld access hole
[20]	DBT-1A-99-176	W30x99 A572 Gr. 50 L_b=138" F_{y-w} = 61.6 ksi F_{u-w} = 82.8 ksi	W14x176 A572 Gr. 50 L_c=168" F_{y-w} =55.6 ksi F_{u-w} =70.7 ksi	SS-FCAW E70TG-K2; backing bar removed at bottom flange	Bolted: 7-1" A325	Tapered cut L_1=7.5" L_{RBS}=20.25" FR=45%	2.8	no failure; test stopped due to limitations in test setup

Ref	Spec.	Beam	Column	Flange Welds	Web Connection	RBS Details and Other Flange Modifications	θ_p (%)	Comments
[20]	DBT-1B-99-176	W30x99 A572 Gr. 50 L_b=138" $F_{y\text{-}w}$ = 51.5 ksi $F_{u\text{-}w}$ = 72.1 ksi	W14x176 A572 Gr. 50 L_c=168" $F_{y\text{-}w}$ =55.5 ksi $F_{u\text{-}w}$ =71.8 ksi	"	"	Tapered cut L_1=7.5" L_{RBS}=20.25" FR=45%	4.0	no failure; test stopped due to limitations in test setup
[20]	DBT-2A-150-257	W36x150 A572 Gr. 50 L_b=138" $F_{y\text{-}w}$ = 60.2 ksi $F_{u\text{-}w}$ = 72.3 ksi	W14x257 A572 Gr. 50 L_c=168" $F_{y\text{-}w}$ =59.6 ksi $F_{u\text{-}w}$ =75.2 ksi	"	Bolted: 9-1" A325	Tapered cut L_1=9" L_{RBS}=24" FR=45%	3.5	Fracture of beam top flange near groove weld
[20]	DBT-2B-150-257	W36x150 A572 Gr. 50 L_b=138" $F_{y\text{-}w}$ = 62.9 ksi $F_{u\text{-}w}$ = 83.1 ksi	W14x257 A572 Gr. 50 L_c=168" $F_{y\text{-}w}$ =64.5 ksi $F_{u\text{-}w}$ =83.2 ksi	"	"	Tapered cut L_1=9" L_{RBS}=24" FR=45%	1.7	Fracture of beam top flange weld; propagated to divot-type fracture of column flange
[10,21]	ARUP-1	W36x150 A572 Gr. 50 L_b=132" $F_{y\text{-}f}$ =55.5 ksi $F_{u\text{-}f}$ =73 ksi $F_{y\text{-}w}$ =62.5 ksi $F_{u\text{-}w}$ =77 ksi	W14x426 A572 Gr. 50 L_c=136"	SS-FCAW E70TG-K2 backing bar left in place w/ seal weld at top flange; backing bar removed at bottom flange	welded (heavy shear tab groove welded to column and fillet welded to beam web)	Tapered cut L_1=9" L_{RBS}=24" FR=44% top & bottom flanges reinforced with vertical ribs	3.5	Flange fracture at minimum section of RBS
[10,21]	COH-1	W27x178 A572 Gr. 50 L_b=132" $F_{y\text{-}f}$ =44 ksi $F_{u\text{-}f}$ =62 ksi $F_{y\text{-}w}$ =46 ksi $F_{u\text{-}w}$ =62 ksi	W14x455 A572 Gr. 50 L_c=136" $F_{y\text{-}f}$ =55 ksi $F_{u\text{-}f}$ =84 ksi $F_{y\text{-}w}$ =54 ksi $F_{u\text{-}w}$ =86 ksi	"	"	Tapered cut L_1=7" L_{RBS}=20" FR=38% top & bottom flanges reinforced with vertical ribs	3.5	"
[10,21]	COH-2	"	"	"	"	"	3.8	"

Ref	Spec.	Beam	Column	Flange Welds	Web Connection	RBS Details and Other Flange Modifications	θ_P (%)	Comments
[10,21]	COH-3	W33x152 A572 Gr. 50 L_b=132" $F_{y\text{-}f}$=57.6 ksi $F_{u\text{-}f}$=78.5 ksi $F_{y\text{-}w}$=62 ksi $F_{u\text{-}w}$=84.5 ksi	W14x455 A572 Gr. 50 L_c=136" $F_{y\text{-}f}$=55 ksi $F_{u\text{-}f}$=84 ksi $F_{y\text{-}w}$=54 ksi $F_{u\text{-}w}$=86 ksi Beam connected to column web	"	"	Tapered cut L_1=9" L_{RBS}=26" FR=43% top & bottom flanges reinforced with vertical side plates	3.2	"
[10,21]	COH-4	"	"	"	"	"	4.0	"
[10,21]	COH-5	W33x152 A572 Gr. 50 L_b=132" $F_{y\text{-}f}$=62.8 ksi $F_{u\text{-}f}$=86 ksi $F_{y\text{-}w}$=69.1 ksi $F_{u\text{-}w}$=93.7 ksi	"	"	"	"	1.8	"
[2,3]	DB1	W36x160 L_b=134" $F_{y\text{-}f}$=54.7 ksi $F_{u\text{-}f}$=75.6 ksi $F_{y\text{-}w}$=53.5 ksi $F_{u\text{-}w}$=79.2 ksi	W14x426 A572 Gr. 50 L_c=136"	SS-FCAW E71T-8 backing bar left in place w/ seal weld at top flange; backing bar removed at bottom flange	welded (beam web groove welded to column)	Constant cut L_1=9" L_{RBS}=19.5" FR=40%	2.0	Flange fracture at RBS
[2,3]	DB2	W36x150 L_b=134" $F_{y\text{-}f}$=41.4 ksi $F_{u\text{-}f}$=58.7 ksi $F_{y\text{-}w}$=47.1 ksi $F_{u\text{-}w}$=61.8 ksi	W14x426 A572 Gr. 50 L_c=136" $F_{y\text{-}f}$=50 ksi $F_{u\text{-}f}$=74.5 ksi $F_{y\text{-}w}$=50 ksi $F_{u\text{-}w}$=75 ksi	"	"	Radius cut L_1=9" L_{RBS}=27" FR=40%	3.0	Testing stopped due to limitations of test setup
[2,3]	DB3	W36x170 L_b=134" $F_{y\text{-}f}$=58 ksi $F_{u\text{-}f}$=73 ksi $F_{y\text{-}w}$=58.5 ksi $F_{u\text{-}w}$=76.7 ksi	W14x426 A572 Gr. 50 L_c=136"	"	"	Radius cut L_1=9" L_{RBS}=27" FR=40%	3.8	"

Ref	Spec.	Beam	Column	Flange Welds	Web Connection	RBS Details and Other Flange Modifications	θ_P (%)	Comments
[2,3]	DB4	W36x194 L_b=134" $F_{y\text{-}f}$=38.5 ksi $F_{u\text{-}f}$=58.6 ksi $F_{y\text{-}w}$=43.6 ksi $F_{u\text{-}w}$=59.8 ksi	W14x426 A572 Gr. 50 L_c=136" $F_{y\text{-}f}$=50 ksi $F_{u\text{-}f}$=74.5 ksi $F_{y\text{-}w}$=50 ksi $F_{u\text{-}w}$=75 ksi	"	"	Radius cut L_1=9" L_{RBS}=27" FR=38%	3.7	"
[2,3]	DB5	W30x148 L_b=134" $F_{y\text{-}f}$=46.6 ksi $F_{u\text{-}f}$=64.5 ksi $F_{y\text{-}w}$=48.5 ksi $F_{u\text{-}w}$=65.4 ksi	W14x257 A572 Gr. 50 L_c=136" $F_{y\text{-}f}$=48.7 ksi $F_{u\text{-}f}$=69 ksi $F_{y\text{-}w}$=49.4 ksi $F_{u\text{-}w}$=66.2 ksi	"	"	Radius cut L_1=5" L_{RBS}=25" FR=38%	4.0	Testing stopped due to limitations of test setup; significant column panel zone yielding
[22]	DB1	W36x135 A36 Steel L_b=134.5"	W14x257 with 1-5/16" thk. cover plates (cover plates welded across flanges of W14x257 to form box) A572 Gr. 50 L_c=132"	SS-FCAW E71T-8 (details of backing and weld tabs not available)	Not Available	Radius cut L_1=8" L_{RBS}=28" FR=40%	3.0	Testing stopped due to limitations of test setup
[23]	S-1	W530x82 (Canadian Designation) d=20.8", b_f=8.2", t_f=0.52", t_w=0.37" wt.=54 lb/ft. L_b=142" CSA G40.41-350W steel $F_{y\text{-}f}$=52.4 ksi $F_{u\text{-}f}$=76.6 ksi $F_{y\text{-}w}$=57.5 ksi $F_{u\text{-}w}$=81 ksi	W14x120 A572 Gr. 50 L_c=120"	SS-FCAW E71T-8 backing bar left in place w/ seal weld at top flange; backing bar removed at bottom flange	Bolted: 5-1" A325	Radius cut L_1=4.7" L_{RBS}=15.7" FR=55%	9.0	Specimen loaded monotonically; testing stopped due to limitations of test setup

Ref	Spec.	Beam	Column	Flange Welds	Web Connection	RBS Details and Other Flange *Modifications*	θ_p (%)	Comments
[23]	S-2A	"	"	"	"	"	3.6	Testing stopped due to limitations of test setup
[23]	SC-1	"	"	"	"	"	3.4	Composite slab included (6); testing stopped due to limitations of test setup
[23]	S-3	"	"	"	"	"	note (8)	statically applied simulated earthquake loading (7); testing stopped due to reaching end of simulated earthquake loading; no connection failure
[23]	S-4	"	"	"	"	"	note (9)	dynamically applied simulated earthquake loading (7); testing stopped due to reaching end of simulated earthquake loading; no connection failure
[23]	SC-2	"	"	"	"	"	Note (9)	Composite slab included (6); dynamically applied simulated earthquake loading (6); testing stopped due to reaching end of simulated earthquake loading; no connection failure

Ref	Spec.	Beam	Column	Flange Welds	Web Connection	RBS Details and Other Flange Modifications	θ_P (%)	Comments
[26]	LS-1	W30x99 A572 Gr. 50 L_b = 141"	W14x176 A572 Gr. 50 L_c = 150"	SS-FCAW E70T-6 backing bar left in place w/ seal weld at top flange; backing bar removed at bottom flange	welded (beam web groove welded to column)	Radius cut L_1=7" L_{RBS}=20" FR=50%	4.0	No connection failure
[26]	LS-2	"	"	"	"	"	+1.0/ -5.0	note (12)
[26]	LS-3	"	"	"	"	"	- 1.0/+ 5.0	note (12)

Notes:

1. All specimens are single cantilever type.
2. All specimens are bare steel, except SC-1 and SC-2
3. All specimens subject to quasi static cyclic loading, with ATC-24 or similar loading protocol, except S-1, S-3, S-4, SC-2, LS-1 and LS-2
4. All specimens provided with continuity plates at beam-to-column connection, except Popov Specimen DB1 (Popov Specimen DB1 was provided with external flange plates welded to column).
5. Specimens ARUP-1, COH-1 to COH-5, S-1, S-2A, S-3, S-4, SC-1 and SC-2 provided with lateral brace near loading point and an additional lateral brace near RBS; all other specimens provided with lateral brace near loading point only.
6. Composite slab details for Specimens SC-2 and SC-2: 118" wide floor slab; 3" ribbed deck (ribs perpendicular to beam) with 2.5" concrete cover; normal wt. concrete; welded wire mesh reinforcement; ¾" dia. shear studs spaced at 24" (one stud in every other rib); first stud located at 29" from face of column; 1" gap left between face of column and slab to minimize composite action.
7. Specimens S-3, S-4 and SC-2 were subjected to simulated earthquake loading based on N10E horizontal component of the Llolleo record from the 1985 Chile Earthquake. For Specimen S-3, simulated loading was applied statically. For Specimen S-4 and SC-2; simulated loading was applied dynamically, and repeated three times.
8. Specimen S-3: Connection sustained static simulated earthquake loading without failure. Maximum plastic rotation demand on specimen was approximately 2%.
9. Specimens S-4 and SC-2: Connection sustained dynamic simulated earthquake loading without failure. Maximum plastic rotation demand on specimen was approximately 2%.
10. Tests conducted by Plumier not included in Table. Specimens consisted of HE 260A beams (equivalent to W10x49) and HE 300B columns (equivalent to W12x79). All specimens were provided with constant cut RBS. Beams attached to columns using fillet welds on beam flanges and web, or using a bolted end plate. Details available in Refs. 24 and 25.

11. Shaking table tests were conducted by Chen, Yeh and Chu [19] on a 0.4 scale single story moment frame with RBS connections. Frame sustained numerous earthquake records without fracture at beam-to-column connections.
12. Specimens LS-2 and LS-3 were tested using near-field loading protocal; The specimen was subjected to peak pulses corresponding to 6% of the story drift ratio six times for LS-2 and four times for LS-3. The specimens eventually failed due to low-cycle fatigue type of fracture at the narrowest section in the beam

Notation:

$F_{y\text{-}f}$ = flange yield stress from coupon tests; $F_{u\text{-}f}$ = flange ultimate stress from coupon tests
$F_{y\text{-}w}$ = web yield stress from coupon tests; $F_{u\text{-}w}$ = web ultimate stress from coupon tests
L_b = Length of beam, measured from load application point to face of column
L_c = Length of column
L_1 = distance from face of column to start of RBS cut
L_{RBS} = length of RBS cut
FR = Flange Reduction = (area of flange removed/original flange area) x100 (Flange Reduction reported at narrowest section of RBS)
θ_P = Maximum plastic rotation developed for at least one full cycle of loading, measured with respect to the face of the column (based on occurrence of fracture or based on the end of loading).